Geol. Mag. **147** (*2*), *2010, pp. 161–170.* © *Cambridge University Press 2009*
doi:10.1017/S0016756809990379

Zoned olivine xenocrysts in a late Mesozoic gabbro from the southern Taihang Mountains: implications for old lithospheric mantle beneath the central North China Craton

JI-FENG YING*, HONG-FU ZHANG & YAN-JIE TANG

State Key Laboratory of Lithospheric Evolution, Institute of Geology and Geophysics, Chinese Academy of Sciences, P.O. Box 9825, Beijing 100029, China

(*Received* 8 April 2009; *accepted* 26 May 2009; First published online 20 August 2009)

Abstract – Zoned olivine grains are abundant in the late Mesozoic Shatuo gabbro (southern Taihang Mountains, central North China Craton). Olivine cores are rich in MgO and NiO, rims are rich in FeO and MnO, and both cores and rims have very low CaO contents. The cores invariably have a high Mg no. (92–94), similar to olivine xenocrysts from Palaeozoic kimberlites in eastern China. The compositional features of these olivines imply that they are xenocrysts rather than phenocrysts, namely, disaggregates of mantle peridotites at the time of intrusion. The compositional similarity of olivine cores to xenocrysts from Palaeozoic kimberlites suggests that the lithospheric mantle beneath the central North China Craton is ancient and refractory in nature, and quite different from eastern China, where the mantle is mainly composed of newly accreted materials resulting from large-scale lithospheric removal and replacement. The contrasting features of the lithospheric mantle beneath the eastern and central North China Craton imply that the large-scale lithospheric removal in Phanerozoic times was mainly confined to the eastern North China Craton.

Keywords: olivine, xenocryst, gabbro, lithospheric mantle, Taihang Mountains.

1. Introduction

Mantle xenoliths in volcanic rocks provide snapshots of the lithospheric mantle at the time of eruption, and direct evidence for the nature of the mantle. Thus, mantle xenoliths are of immense value in deciphering the nature and evolution of the lithosphere (Nixon, 1987; Pearson, Canil & Shirey, 2003). Mantle-derived xenocrysts in volcanic rocks, such as garnet, olivine, clinopyroxene and chromite, derived from disaggregated mantle xenoliths, also bear information about the protolith and can be used to extract information about the chemical nature and processes of the lithospheric mantle (Griffin *et al.* 1999; Scully, Canil & Schulze, 2004; Zhang, 2005; Zhang *et al.* 2007), especially in regions where mantle xenoliths are not available. Here, we describe zoned olivine xenocrysts that are widely distributed in a gabbroic intrusion from the southern Taihang Mountains, north China, and present detailed compositions of these olivine xenocrysts. Further, we discuss the compositional characteristics and evolution of the sub-continental lithospheric mantle beneath the North China Craton.

2. Geological setting and petrography

The North China Craton, with its Archaean to early Proterozoic basement, is the largest and oldest craton in China (Jahn *et al.* 1987; Liu *et al.* 1992). Geological and geophysical observations reveal that the North China Craton is traversed by two large-scale N–S-trending linear zones: the Tan-Lu Fault in the east, and the Daxing'anling–Taihang gravity lineament in the west (Ma, 1989; Menzies & Xu, 1998) (Fig. 1). The Daxing'anling–Taihang gravity lineament was traditionally regarded as the boundary between the eastern and western parts of the North China Craton. The regions to the west of the Daxing'anling–Taihang gravity lineament are characterized by thick crust (> 40 km) and lithosphere (> 100 km), large negative Bouguer gravity anomalies and low heat flow. In contrast, the regions to the east of the Daxing'anling–Taihang gravity lineament have much thinner crust (< 35 km) and lithosphere (60–80 km), Bouguer gravity anomalies are weakly negative to positive and heat flow is relatively high (Ma, 1989; Hu, He & Wang, 2000; Chen *et al.* 2008). The North China Craton can also be divided into three parts, according to lithological and geochemical studies, and metamorphic *P–T–t* paths of the basement rocks, namely the Eastern and Western blocks and the Trans-North China Orogen (also called the Central Zone) (Zhao *et al.* 2001) (Fig. 1). The Eastern Block is composed of early to late Archaean orthogneisses intruded by 2.5 Ga syntectonic granitoids. The Western Block consists of Archaean basement with overlying Archaean to Palaeoproterozoic metasediments (Li *et al.* 2000; Zhao *et al.* 2000). The Trans-North China Orogen is composed of late Archaean amphibolites, granulites and greenstones overlain by bimodal volcanic rocks and terrigenous sedimentary rocks. It was generally considered that

*Author for correspondence: jfying@mail.iggcas.ac.cn

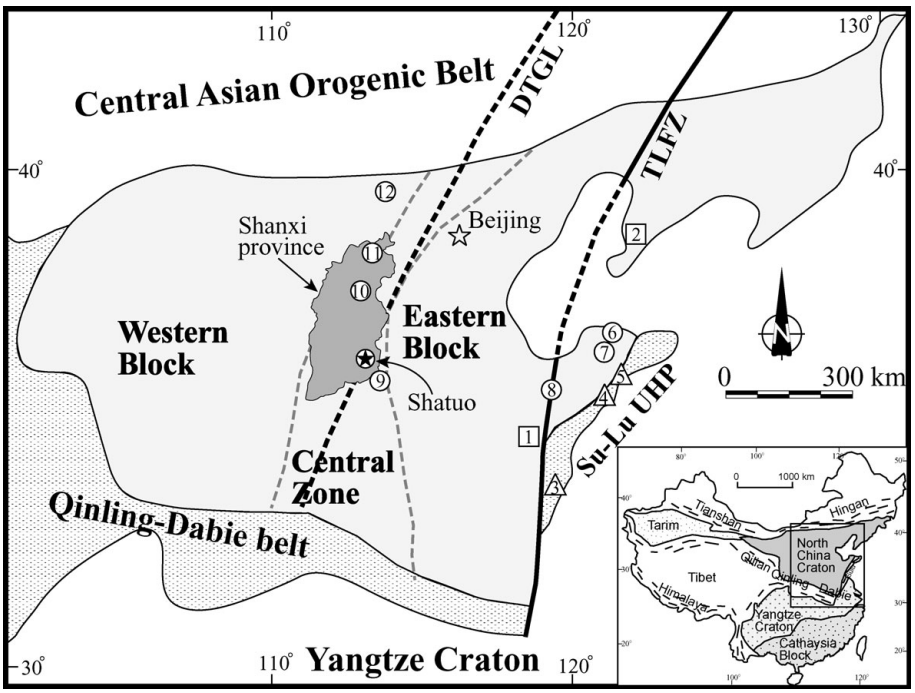

Figure 1. Simplified geological map showing the major tectonic units in eastern China and the location of the Shatuo gabbro; the locations of Palaeozoic kimberlites (open squares) and Mesozoic (open triangles) and Cenozoic (open circles) xenolith-bearing basalts are also marked. 1 – Mengyin kimberlites; 2 – Fuxian kimberlites; 3 – Junan basalts; 4 – Jiaozhou basalts; 5 – Qingdao basalts; 6 – Penglai basalts; 7 – Qixia basalts; 8 – Changle basalts; 9 – Hebi basalts; 10 – Fansi basalts; 11 – Yangyuan basalts; 12 – Hanuoba basalts. Note that the North China Craton is traversed by two large-scale N–S-trending linear zones, namely, the Tan-Lu fault zone (TLFZ) to the east and the Daxinganling–Taihang gravity lineament (DTGL) to the west. Two shaded dashed lines outline the three-fold tectonic division of the North China Craton (after Zhao *et al.* 2001). Inset shows location of the North China Craton relative to other cratonic blocks and intervening fold belts.

the Eastern and Western blocks evolved independently from late Archaean to early Palaeoproterozoic times before colliding into a coherent craton along the Trans-North China Orogen at *c.* 1.85 Ga (Zhao *et al.* 2000, 2001).

The southern Taihang Mountain is a part of the Trans-North China Orogen of the North China Craton. Mesozoic intrusive complexes are widely distributed in this region, with a range of rock types including gabbros, hornblende diorites, syenites and monzonites. The gabbro outcrops are generally small (usually less than 0.5 km^2) and occur as knobs or xenoliths hosted by hornblende diorites (Shanxi Bureau of Geology and Mineral Resources, 1982). The samples in this study were collected from the Shatuo gabbro in Huguan county, Shanxi Province. Gabbroic samples are fresh, dark grey and medium- to coarse-grained rocks, composed of plagioclase (40–50 %), clinopyroxene (20 %), olivine (5–10 %), biotite (10 %), amphibole (5 %) and alkali feldspar (5 %). Accessory phases include zircon, sphene, apatite and Fe–Ti oxides. Analyses of zircons extracted from gabbro using a Cameca 1280 secondary ion mass spectrometer yielded a concordant U–Pb age of 128.4 ± 1.2 Ma (Ying *et al.* unpub. data). Olivines are generally rounded and have varied grain size (from < 1–8 mm). All olivine grains show compositional zonation in backscattered electron images (BSE), with darker Mg-rich cores and lighter Fe-rich rims (Fig. 2).

3. Analytical methods

The mineral chemistry of olivine was obtained with a JEOL Superprobe at the Institute of Geology and Geophysics, Chinese Academy of Sciences. The analyses were operated at 15 kv accelerating voltage, 10 nA beam current and 2 μm beam diameter. The counting time varied between 10 and 30 seconds for different elements. Natural mineral standards were used for calibration.

4. Olivine chemistry

As shown in backscattered electron images, the olivine grains exhibit apparent zonation and span a wide compositional range (Table 1). The cores invariably have higher MgO and NiO contents and lower FeO and MnO contents than the rims, and the compositional change towards the rims is gradual (Fig. 3). The Mg nos of cores are generally higher than 91 and the highest can reach to 94 (sample 02ST-9). The rims have variable compositions, with Mg no. ranging from 79 to 89 (Table 1). The cores and the rims show comparable and low CaO concentrations (< 0.1 wt %).

5. Discussion

5.a. Are zoned olivines phenocrysts or xenocrysts?

Both olivine phenocrysts and xenocrysts are common in volcanic rocks (Hirano *et al.* 2004; Zhang *et al.*

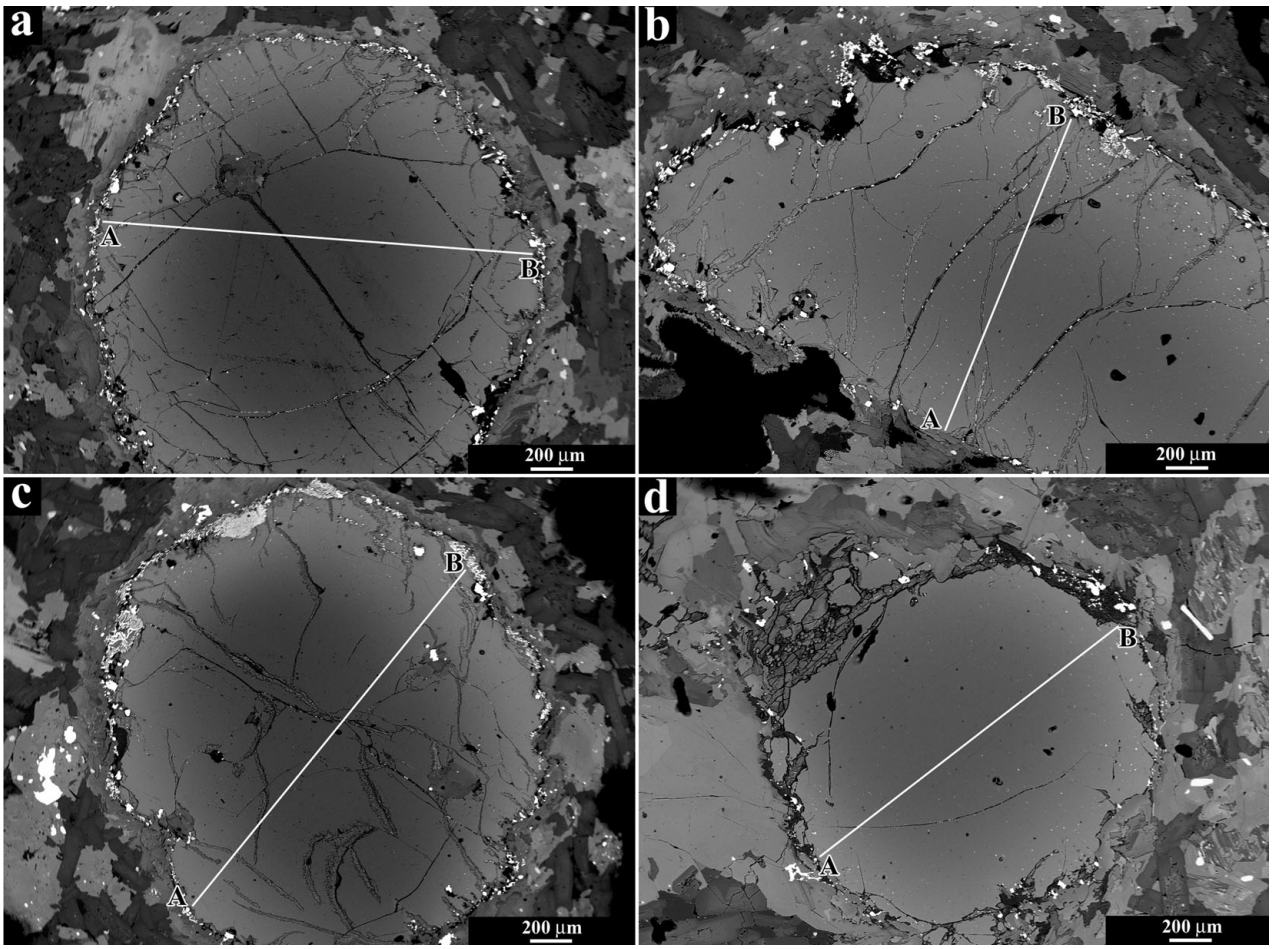

Figure 2. Backscattered electron images (BSE) of zoned olivine xenocrysts; traverse lines analysed by electron probe micro-analysis are also shown. (a) SG03.1, (b) SG03.2, (c) SG02, (d) 02ST-5.

2004*b*; Zhang, 2005). Phenocrysts are genetically related to the host magma and usually crystallized in the magma chamber prior to magma eruption; in contrast, no genetic relationship exists between the host magma and xenocrysts, and the latter were considered to be entrained in the host magma during the volcanic eruption or magmatic intrusion.

It has been observed that olivines of magmatic origin usually have higher CaO contents (> 0.2 %) than those in mantle xenoliths (Gurenko, Hansteen & Schmincke, 1996; Thompson & Gibson, 2000), though some low-Ca olivine phenocrysts were found recently in some subduction-related magmas, and such low-Ca olivines were usually characterized by the presence of melt inclusions (Kamenetsky *et al.* 2006; Elburg & Kamenetsky, 2008). The olivine grains in this study show very low CaO contents regardless of cores or rims (Fig. 4); in addition, melt inclusions were not observed in all olivine grains, so it can be ruled out that these olivines are crystallizing phases of host magma, namely phenocrysts. Moreover, a simple calculation shows that the forsterite content of olivines in equilibrium with the host magma should be no more than 91 (Fig. 5), far lower than that of the olivine cores; therefore, these olivines are disaggregated from mantle xenoliths rather than magmatic phenocrysts. As a result, these olivine xenocrysts can be used to constrain the nature of the lithospheric mantle beneath that region at the time of the gabbroic intrusion.

5.b. Formation of the zoned olivine xenocrysts

Olivine xenocrysts, which were almost neglected in previous studies, have been widely observed recently in the late Mesozoic and Cenozoic basalts from both eastern and western parts of the North China Craton, and all xenocrysts found invariably show zoned texture (Pei *et al.* 2004; Tang, Zhang & Ying, 2004; Zhang *et al.* 2004*b*; Shao *et al.* 2005; Zhang, 2005). Because other mineral phases in the gabbros are not zoned, the zonation texture induced by late-stage magmatic fluid infiltration or post-emplacement processes can be ruled out, and we attribute the chemical zonation texture in olivines to re-equilibration through diffusional exchange between the olivine and host magma (Maaløe & Hansen, 1982; Nakamura, 1995; Larsen & Pedersen, 2000; Klugel, 2001). When olivine crystals are entrapped in high-temperature basaltic magma, the chemical disequilibrium between olivine and host magma will cause a reaction and chemical exchange, and the degree of re-equilibration depends on the size of the olivine and the duration

Table 1. Representative analyses of olivine xenocrysts from Mesozoic Shatuo gabbros

Olivine	μm	SiO_2	Cr_2O_3	FeO	MnO	MgO	CaO	NiO	Mg no.
Line analyses									
	A	39.42	0.00	18.94	0.48	40.98	0.03	0.25	79.6
	50	35.58	0.11	18.19	0.36	37.39	0.15	0.32	78.7
	100	39.71	0.00	18.54	0.38	41.57	0.05	0.33	80.1
	150	39.63	0.02	17.69	0.32	42.06	0.10	0.28	81.1
	200	39.71	0.00	16.69	0.31	42.85	0.03	0.33	82.2
	250	40.23	0.02	14.10	0.25	45.03	0.04	0.37	85.2
	300	40.20	0.01	12.99	0.22	45.37	0.08	0.35	86.3
	350	40.48	0.06	11.66	0.19	47.18	0.03	0.36	87.9
	400	40.60	0.07	10.46	0.13	47.82	0.07	0.39	89.2
	450	40.95	0.01	9.67	0.14	48.23	0.06	0.39	90.0
	500	40.94	0.02	8.94	0.10	48.55	0.07	0.39	90.7
	550	40.87	0.05	8.60	0.09	49.17	0.05	0.38	91.1
	600	41.09	0.05	8.08	0.10	49.53	0.05	0.38	91.7
	650	41.65	0.06	8.06	0.10	49.76	0.09	0.41	91.7
	700	41.37	0.07	7.70	0.10	50.02	0.07	0.35	92.1
	750	41.56	0.03	7.65	0.06	49.58	0.07	0.37	92.1
	800	41.06	0.06	7.86	0.11	49.88	0.05	0.44	92.0
	850	41.21	0.08	7.66	0.08	49.30	0.09	0.41	92.1
	900	41.09	0.02	7.85	0.11	50.05	0.08	0.33	92.0
	950	41.11	0.05	7.67	0.10	49.74	0.06	0.39	92.1
SG03.1	1000	41.13	0.03	7.80	0.08	48.13	0.04	0.34	91.7
	1050	41.24	0.03	8.08	0.09	49.53	0.15	0.38	91.7
	1100	41.34	0.04	8.12	0.10	49.58	0.10	0.39	91.7
	1150	41.10	0.02	8.17	0.13	49.08	0.10	0.37	91.5
	1200	36.13	0.04	8.18	0.08	44.27	0.04	0.34	90.7
	1250	41.01	0.05	8.93	0.12	49.01	0.05	0.36	90.8
	1300	41.02	0.03	9.04	0.13	48.38	0.08	0.37	90.6
	1350	40.63	0.03	9.59	0.10	48.38	0.06	0.34	90.1
	1400	40.82	0.01	10.00	0.10	48.32	0.06	0.36	89.7
	1450	40.53	0.00	10.61	0.19	47.79	0.04	0.36	89.0
	1500	40.22	0.00	11.17	0.12	46.81	0.06	0.32	88.3
	1550	40.05	0.02	11.94	0.14	46.54	0.08	0.32	87.5
	1600	39.76	0.00	12.67	0.20	45.75	0.05	0.33	86.7
	1650	39.94	0.04	13.26	0.19	45.18	0.09	0.31	86.0
	1700	39.83	0.00	14.04	0.25	44.55	0.06	0.32	85.1
	1750	38.77	0.05	15.55	0.27	44.38	0.06	0.30	83.7
	1800	39.31	0.01	16.00	0.32	43.06	0.08	0.34	82.9
	1850	38.64	0.02	17.27	0.38	41.81	0.08	0.26	81.3
	1900	38.58	0.00	17.85	0.41	41.57	0.04	0.29	80.7
	1950	38.85	0.04	18.77	0.41	41.01	0.07	0.30	79.7
	B	38.62	0.00	18.98	0.51	40.51	0.03	0.34	79.3
	A	38.87	0.06	16.64	0.38	42.85	0.04	0.37	82.3
	125	39.81	0.00	12.49	0.18	45.86	0.03	0.34	86.9
	250	40.43	0.02	9.25	0.16	48.28	0.04	0.41	90.4
	375	40.42	0.03	8.46	0.12	48.91	0.07	0.39	91.2
02ST-5	500	40.66	0.02	8.21	0.12	49.03	0.10	0.32	91.5
	625	40.36	0.02	8.44	0.11	48.97	0.06	0.33	91.3
	750	40.38	0.07	9.35	0.11	48.78	0.07	0.37	90.4
	875	39.71	0.01	12.03	0.22	46.27	0.08	0.35	87.4
	B	38.66	0.02	15.76	0.32	43.11	0.05	0.31	83.1
	A	38.69	0.02	19.02	0.42	41.09	0.05	0.26	79.5
	65	38.97	0.04	17.53	0.36	41.86	0.07	0.27	81.1
	130	39.35	0.03	16.54	0.35	43.99	0.05	0.32	82.7
	195	39.42	0.01	14.55	0.27	44.32	0.04	0.31	84.6
	260	39.64	0.00	13.70	0.23	44.90	0.04	0.29	85.5
	325	39.76	0.03	13.29	0.21	45.34	0.07	0.35	86.0
	390	40.21	0.00	12.85	0.21	45.57	0.06	0.28	86.5
	455	40.17	0.06	12.69	0.24	45.83	0.08	0.37	86.7
SG03.2	520	40.00	0.04	13.00	0.21	45.70	0.05	0.34	86.4
	585	40.20	0.01	13.42	0.24	45.42	0.01	0.31	85.9
	650	40.06	0.02	13.81	0.25	45.02	0.06	0.30	85.4
	715	39.96	0.03	14.57	0.22	44.05	0.06	0.27	84.5
	780	39.68	0.03	15.60	0.27	43.51	0.06	0.32	83.4
	845	39.67	0.02	16.64	0.33	42.66	0.12	0.33	82.2
	910	39.16	0.06	17.51	0.35	42.03	0.07	0.25	81.2
	975	39.21	0.04	18.70	0.42	41.46	0.07	0.28	80.0
	B	39.10	0.01	18.26	0.50	40.99	0.06	0.22	80.2
	A	38.46	0.02	19.24	0.42	40.97	0.03	0.28	79.3
	150	39.07	0.02	16.93	0.29	42.09	0.06	0.28	81.7
	300	41.18	0.04	14.48	0.23	46.40	0.05	0.28	85.2
	450	40.63	0.01	11.68	0.14	45.77	0.05	0.25	87.6
	600	40.33	0.00	10.49	0.16	47.40	0.07	0.32	89.0
	750	41.52	0.00	9.01	0.06	50.46	0.06	0.34	91.0
	900	40.86	0.00	8.52	0.11	49.17	0.07	0.38	91.2

Table 1. (*Cont.*)

Olivine	μm	SiO_2	Cr_2O_3	FeO	MnO	MgO	CaO	NiO	Mg no.
SG02	1050	41.10	0.04	8.57	0.10	48.56	0.02	0.36	91.1
	1200	40.85	0.02	8.80	0.13	49.16	0.08	0.36	91.0
	1350	41.66	0.04	10.80	0.15	48.24	0.06	0.34	88.9
	1500	39.99	0.14	12.58	0.21	45.59	0.07	0.31	86.7
	1650	42.15	0.17	14.94	0.25	42.89	0.09	0.28	83.8
	1800	39.49	0.00	18.09	0.33	41.76	0.07	0.27	80.6
	B	38.83	0.00	19.31	0.42	39.90	0.06	0.27	78.8
	core	40.72	0.06	6.32	0.01	51.46	0.07	0.43	93.6
	core	40.32	0.06	6.15	0.07	51.90	0.05	0.52	93.8
	core	40.08	0.07	6.22	0.05	51.52	0.04	0.47	93.7
	mantle	40.78	0.02	6.23	0.02	51.06	0.06	0.38	93.7
02ST-9	mantle	40.39	0.01	6.38	0.08	51.12	0.07	0.44	93.5
	mantle	40.89	0.03	6.10	0.06	51.10	0.05	0.39	93.8
	rim	39.77	0.06	10.29	0.18	48.25	0.02	0.37	89.4
	rim	39.07	0.00	11.69	0.18	46.39	0.03	0.40	87.7
02ST-11	core	40.74	0.03	7.55	0.13	49.75	0.10	0.36	92.2
Grain 1	mantle	39.59	0.02	10.09	0.16	47.88	0.03	0.30	89.5
	rim	39.44	0.00	13.82	0.28	44.84	0.03	0.28	85.4
02ST-11	core	40.37	0.03	7.18	0.09	50.19	0.04	0.35	92.6
Grain 2	mantle	40.67	0.05	9.17	0.13	48.49	0.02	0.33	90.5
	rim	39.69	0.01	13.68	0.27	45.48	0.04	0.38	85.7

of the reaction. The bigger the olivine xenocrysts are, the wider the compositional gradients that exist between the cores and rims. For example, the olivine in sample 02ST-9 is the biggest grain in this study (with diameter up to 8 mm) (Table 1), and it exhibits the largest core–rim variations in Mg no. (94–87). As shown by the line analyses of olivine xenocrysts, the chemical variation between the cores and rims is mainly manifested in the Fe and Mg differences, since Mg and Fe diffusion in olivine is rapid (Mg diffusion coefficient in olivine is around 1.4×10^{-8} cm^2 s^{-1}: Brearley & Scarfe, 1986; Redfern *et al.* 1996; Chakraborty, 1997). As a result, preservation of the zoned olivine xenocrysts requires the reaction duration to be short. Since Mn has a comparable diffusion coefficient to Mg–Fe, while the diffusion coefficient of Ca is about 1 order of magnitude slower than that for Mg–Fe diffusion in olivine (Chakraborty, 1997; Coogan *et al.* 2005), the compositional zonation is also apparent in terms of Mn, while there is no measurable zonation of Ca on such a short timescale. It is also worth noting that the Mg no. of the olivine xenocryst rims should be equal or close to that of calculated olivine equilibrating with gabbro, however, this is not what we observed; the rims are much less Mg-rich than expected for bulk equilibrium (Fig. 5). The likely explanation is that when we calculated the equilibrating olivine using whole rock compositions, the olivine xenocrysts were not excluded, which definitely increased the Mg no. of the whole rocks and the subsequent calculated olivine values. Furthermore, olivine xenocrysts described in basalts elsewhere (Tang, Zhang & Ying, 2004; Zhang *et al.* 2004*b*; Shao *et al.* 2005; Zhang, 2005) show much narrower rims than those in the Shatuo gabbro because the reaction durations between olivine xenocrysts and extrusive basalts are considerably shorter than those of intrusive gabbros.

5.c. Implications for the lithospheric mantle evolution of North China Craton

It has been well documented that the North China Craton experienced extensive lithospheric extension during Late Mesozoic to Cenozoic times, which resulted in large-scale removal of lithospheric mantle and significant compositional change of the mantle (Menzies, Fan & Zhang, 1993; Griffin *et al.* 1998; Xu, 2001; Gao *et al.* 2002; Zhang *et al.* 2002). The North China Craton had a thick, cold and highly refractory lithospheric mantle, at least prior to mid-Ordovician times, as indicated by mantle xenoliths, xenocrysts and diamond inclusions entrapped in Palaeozoic kimberlites in Mengyin and Fuxian counties. The Mg nos of olivine xenocrysts in those kimberlites are high (92–95) and comparable to those of olivines from kimberlite-borne peridotitic xenoliths (Zheng *et al.* 2001). Such highly refractory mantle peridotites have been widely replaced by fertile mantle peridotites since Mesozoic times, and olivines in those peridotites are less magnesian (Mg no. < 91) (Menzies, Fan & Zhang, 1993; Griffin *et al.* 1998; Fan *et al.* 2000; Xu, 2001). It is worth noting, however, that these observations were mostly confined to the eastern part of the North China Craton; the nature and evolution of lithosphere in the central and western parts of the North China Craton were not well constrained.

As mentioned above, the olivine xenocrysts in the Shatuo gabbro represent disaggregated minerals from the mantle peridotites at the time of gabbroic intrusion, so the olivine xenocrysts can be used to discern the nature of the lithospheric mantle beneath the central North China Craton. The olivine cores from the Shatuo gabbro have a very high Mg no. (> 92), which is similar to those from Palaeozoic kimberlites in eastern China and the olivines from high-Mg peridotites entrained in Mesozoic and Cenozoic basalts (Fig. 6). Re–Os

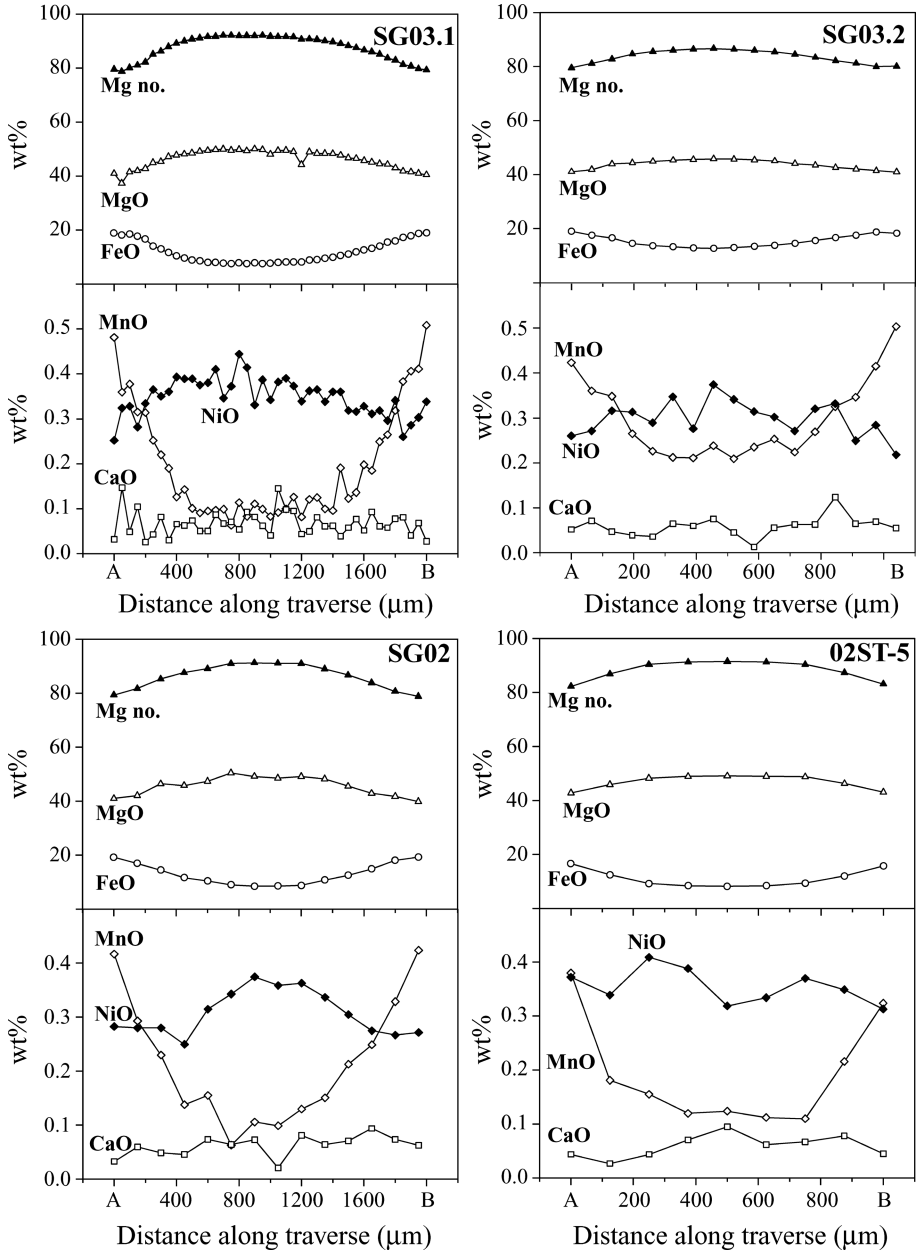

Figure 3. Compositional traverses for four representative olivine xenocrysts.

isotopic studies of the refractory mantle xenoliths entrained in Palaeozoic kimberlites have revealed that the lithospheric mantle is Archaean in age (Gao *et al.* 2002; Wu *et al.* 2006; Zhang *et al.* 2008). The high-Mg peridotite xenoliths in Cenozoic Hebi basalts were interpreted as relics of Archaean lithospheric mantle, confirmed by Re–Os isotopic dating of sulphide inclusions in olivines (Zheng *et al.* 2001, 2006).

Although the Mg no. of olivine actually only reflects the degree of partial melting that the mantle experienced rather than age, there is a correlation between the ages of lithospheric mantle and olivine Mg no. based on the studies of sub-continental peridotite xenoliths entrained in kimberlites, lamproites and basalts from different tectonic regimes. The Mg no. of olivine of Archaean lithospheric mantle is usually greater than 92, those of Proterozoic lithospheric mantle between 91 and 92 and those of the Phanerozoic less than 91 (Griffin, O'Reilly & Ryan, 1999). Such a relationship can be accounted for by the relatively higher degree of partial melting (25–30 %) of the mantle peridotites in the Archaean and Proterozoic due to the higher geothermal gradient at that time. The geothermal gradient in the Phanerozoic was low and the mantle underwent a lower degree of partial melting, which would form less magnesian olivines if no thermal anomaly such as a hot spot or mantle plume was present. Though some highly magnesian olivines in young dunites have been reported, the occurrence of such dunites was only restricted to ophiolites and was small in volume (veins or pods) (Suhr *et al.* 2003), and it is unlikely that the above dunitic olivines are widely distributed in a cratonic lithospheric

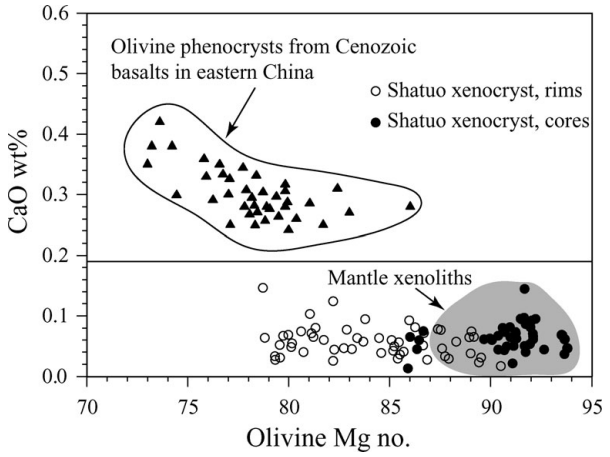

Figure 4. Olivine CaO content versus Mg no. (% forsterite) plot showing the discrimination between phenocrysts crystallized from magma and xenocrysts from disaggregated mantle (Gurenko, Hansteen & Schmincke, 1996; Thompson & Gibson, 2000). Shaded region: olivines from mantle xenoliths included in Palaeozoic kimberlites, Mesozoic and Cenozoic basalts in eastern China (Zheng, 1999; Fan *et al.* 2000; Zheng *et al.* 2001; Yan, Chen & Xie, 2003; Ying *et al.* 2006). Olivine phenocrysts in Cenozoic basalts in eastern China (E & Zhao, 1987; Tang, Zhang & Ying, 2004).

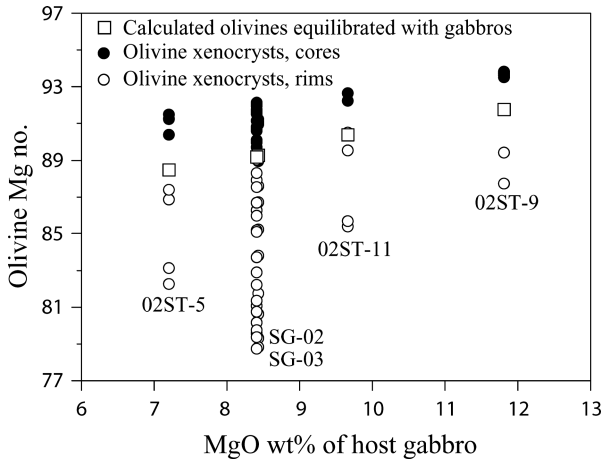

Figure 5. Olivine Mg no. versus MgO contents of whole rocks of the Shatuo gabbro. Fe–Mg partition coefficient of 0.33 between olivine and melt (Ulmer, 1989) was used in calculation. The MgO and FeO contents of the Shatuo gabbro are as follows: SG02: 8.43 wt %, 5.50 wt %; SG03: 8.41 wt %, 5.55 wt %; 02ST-5: 7.20 wt %, 5.10 wt %; 02ST-9: 11.81 wt %, 5.75 wt %; 02ST-11: 9.66 wt %, 5.60 wt %.

mantle. Consequently, it is reasonable to infer that the lithospheric mantle beneath the central North China Craton during late Mesozoic times, as reflected by the olivine xenocrysts, was still refractory and ancient in nature. In addition, all late Mesozoic mafic igneous rocks in the central North China Craton demonstrated the EM I isotopic feature (Chen & Zhai, 2003; Zhang *et al.* 2004*a*; Wang *et al.* 2006), a character shared by cratonic ancient mantle worldwide (Menzies, 1990). Recent Sr, Nd and Os isotopic studies of the peridotite xenoliths from the Cenozoic Yangyuan and Fansi alkali basalts in the central North China Craton provided

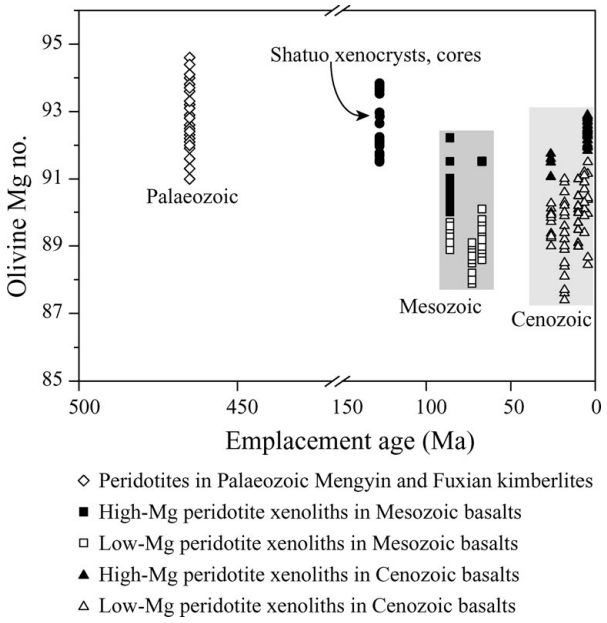

Figure 6. Olivine Mg no. versus emplacement ages of mantle xenolith-bearing volcanic rocks in eastern China. Data sources: E & Zhao, 1987; Zheng, 1999; Fan *et al.* 2000; Zheng *et al.* 2001; Yan, Chen & Xie, 2003; Ying *et al.* 2006; J. Zhang, unpub. Ph.D. thesis, Chinese Acad. Sciences, 2007.

direct evidence that the underlying lithospheric mantle is Archaean or very early Proterozoic (Xu *et al.* 2008).

In contrast to the widespread existence of Archaean lithospheric mantle beneath the central North China Craton in the late Mesozoic and Cenozoic, the lithospheric mantle underneath the eastern North China Craton is predominantly composed of young and newly accreted material (Fan *et al.* 2000; Gao *et al.* 2002; Wu *et al.* 2003), although in some regions ancient mantle residues are still present as shown by the existence of high-Mg peridotite xenoliths (Zheng *et al.* 2001; Ying *et al.* 2006) and Re–Os isotopic data (Gao *et al.* 2002; Wu *et al.* 2006). In addition, geophysical data, such as low heat flow (Hu, He & Wang, 2000) and a negative Bouguer gravity anomaly (Ma, 1989), have also implied a thick, cold lithosphere in the western North China Craton. The contrasting nature of the lithospheric mantle between the eastern and central North China Craton suggests that they had a different evolutionary history in Phanerozoic times; the extensive lithospheric removal which resulted in replacement of the ancient and refractory lithospheric mantle by a young fertile one was mainly confined to the eastern North China Craton, while the lithospheric mantle beneath the central and western North China Craton was weakly affected.

6. Conclusions

The zoned olivine crystals from the late Mesozoic Shatuo gabbro are xenocrysts that disaggregated from mantle peridotites and can be used to discern the nature of the lithospheric mantle at the time of the

gabbro intrusion. The zoned texture was formed by diffusional exchange between olivine and the host melt due to their compositional disequilibria. The compositions of olivine cores represented those of mantle peridotites. The similarities in composition of the olivine cores to those from Palaeozoic kimberlites and high-Mg peridotites imply that the lithospheric mantle beneath the central North China Craton is ancient and refractory, which is in sharp contrast to the prevalent young and newly accreted features of the mantle beneath the eastern North China Craton. The different natures of lithospheric mantle of the eastern and western North China Craton suggest that the extensive lithospheric removal was mainly confined to the eastern North China Craton, while the lithospheric mantle beneath the central North China Craton was weakly affected.

Acknowledgements. We are grateful to Y. G. Ma and Q. Mao for their help with arrangements and assistance in electron microprobe analyses. Dr David Pyle is thanked for his thoughtful suggestions and constructive comments. Mrs J. Holland is also thanked for her helpful editorial efforts. This work was financially supported by the Chinese Academy of Sciences (KZCX2-YW-103).

References

BREARLEY, M. & SCARFE, C. M. 1986. Dissolution rates of upper mantle minerals in an alkali basalt melt at high-pressure – an experimental-study and implications for ultramafic xenolith survival. *Journal of Petrology* **27**, 1157–82.

CHAKRABORTY, S. 1997. Rates and mechanisms of Fe–Mg interdiffusion in olivine at 980–1300°C. *Journal of Geophysical Research, Solid Earth* **102**, 12317–31.

CHEN, B. & ZHAI, M. G. 2003. Geochemistry of late Mesozoic lamprophyre dykes from the Taihang Mountains, north China, and implications for the sub-continental lithospheric mantle. *Geological Magazine* **140**, 87–93.

CHEN, L., TAO, W., ZHAO, L. & ZHENG, T. 2008. Distinct lateral variation of lithospheric thickness in the Northeastern North China Craton. *Earth and Planetary Science Letters* **267**, 56–68.

COOGAN, L. A., HAIN, A., STAHL, S. & CHAKRABORTY, S. 2005. Experimental determination of the diffusion coefficient for calcium in olivine between 900°C and 1500°C. *Geochimica et Cosmochimica Acta* **69**, 3683–94.

E, M. L. & ZHAO, D. S. 1987. *Cenozoic basalts and deep-seated xenoliths in eastern China*. Beijing: Science Press, 490 pp. (in Chinese).

ELBURG, M. & KAMENETSKY, V. S. 2008. Limited influence of subducted continental material on mineralogy and elemental geochemistry of primitive magmas from Indonesia-Australia collision zone. *Lithos* **105**, 73–84.

FAN, W. M., ZHANG, H. F., BAKER, J., JARVIS, K. E., MASON, P. R. D. & MENZIES, M. A. 2000. On and off the North China craton: where is the Archaean keel? *Journal of Petrology* **41**, 933–50.

GAO, S., RUDNICK, R. L., CARLSON, R. W., MCDONOUGH, W. F. & LIU, Y. S. 2002. Re–Os evidence for replacement of ancient mantle lithosphere beneath the North China Craton. *Earth and Planetary Science Letters* **198**, 307–22.

GRIFFIN, W. L., FISHER, N. I., FRIEDMAN, J., RYAN, C. G. & O'REILLY, S. Y. 1999. Cr-pyrope garnets in the lithospheric mantle. I. Compositional systematics and relations to tectonic setting. *Journal of Petrology* **40**, 679–704.

GRIFFIN, W. L., O'REILLY, S. Y. & RYAN, C. G. 1999. The composition and origin of subcontinental lithospheric mantle. In *Mantle Petrology: Field observations and high-pressure experimentation: A tribute to Francis R. (Joe) Boyd* (eds Y. Fei, C. M. Bertka & B. O. Mysen), pp. 13–45. Houston: The Geochemical Society.

GRIFFIN, W. L., ZHANG, A. D., O'REILLY, S. Y. & RYAN, C. G. 1998. Phanerozoic evolution of the lithosphere beneath the Sino-Korean craton In *Mantle dynamics and plate interactions in east Asia* (eds M. Flower, S. L. Chung, C. H. Lo & T. Y. Lee), pp. 107–26. Washington, D.C.: American Geophysical Union.

GURENKO, A. A., HANSTEEN, T. H. & SCHMINCKE, H. U. 1996. Evolution of parental magmas of Miocene shield basalts of Gran Canaria (Canary Islands): constraints from crystal, melt and fluid inclusions in minerals. *Contributions to Mineralogy and Petrology* **124**, 422–35.

HIRANO, N., YAMAMOTO, J., KAGI, H. & ISHII, T. 2004. Young, olivine xenocryst-bearing alkali-basalt from the oceanward slope of the Japan Trench. *Contributions to Mineralogy and Petrology* **148**, 47–54.

HU, S. B., HE, L. J. & WANG, J. Y. 2000. Heat flow in the continental area of China: a new data set. *Earth and Planetary Science Letters* **179**, 407–19.

JAHN, B. M., AUVRAY, B., CORNICHET, J., BAI, Y. L., SHEN, Q. H. & LIU, D. Y. 1987. 3.5 Ga old amphibolites from eastern Hebei Province, China – field occurrence, petrography, Sm–Nd isochron age and REE geochemistry. *Precambrian Research* **34**, 311–46.

KAMENETSKY, V. S., ELBURG, M., ARCULUS, R. & THOMAS, R. 2006. Magmatic origin of low-Ca olivine in subduction-related magmas: Co-existence of contrasting magmas. *Chemical Geology* **233**, 346–57.

KLUGEL, A. 2001. Prolonged reactions between harzburgite xenoliths and silica-undersaturated melt: implications for dissolution and Fe–Mg interdiffusion rates of orthopyroxene. *Contributions to Mineralogy and Petrology* **141**, 1–14.

LARSEN, L. M. & PEDERSEN, A. K. 2000. Processes in high-mg, high-T magmas: Evidence from olivine, chromite and glass in palaeogene picrites from West Greenland. *Journal of Petrology* **41**, 1071–98.

LI, J. H., QIAN, X. L., HUANG, X. N. & LIU, S. W. 2000. Tectonic framework of the North China craton and its cratonization in the early Precambrian. *Acta Petrologica Sinica* **16**, 1–10 (in Chinese with English abstract).

LIU, D. Y., NUTMAN, A. P., COMPSTON, W., WU, J. S. & SHEN, Q. H. 1992. Remnants of ≥ 3800 Ma crust in the Chinese part of the Sino-Korean craton. *Geology* **20**, 339–42.

MA, X. Y. 1989. *Atlas of active faults of China*. Beijing: Seismologic Press, 120 pp. (in Chinese).

MAALØE, S. & HANSEN, B. 1982. Olivine phenocrysts of Hawaiian olivine tholeiite and oceanite. *Contributions to Mineralogy and Petrology* **81**, 203–211.

MENZIES, M. A. 1990. *Continental mantle*. Oxford: Clarendon Press, 184 pp.

MENZIES, M. A., FAN, W. M. & ZHANG, M. 1993. Paleozoic and Cenozoic lithoprobes and the loss of >120 km of Archean lithosphere, Sino-Korean craton, China. In *Magmatic processes and plate tectonics* (eds H. M. Prichard, T. Alabaster, N. B. W. Harris & C. R. Neary),

pp. 71–81. Geological Society of London, Special Publication no. 76.

MENZIES, M. A. & XU, Y. G. 1998. Geodynamics of the North China craton. In *Mantle Dynamics and Plate Interactions in East Asia* (eds M. F. J. Flower, S. L. Chung, C. H. Lo & T. Y. Lee), pp. 155–65. American Geophysical Union.

NAKAMURA, M. 1995. Residence time and crystallization history of nickeliferous olivine phenocrysts from the northern Yatsugatake volcanoes, Central Japan: Application of a growth and diffusion model in the system Mg–Fe–Ni. *Journal of Volcanology and Geothermal Research* **66**, 81–100.

NIXON, P. H. 1987. *Mantle xenoliths*. Chichester: John Wiley & Sons, 844 pp.

PEARSON, D. G., CANIL, D. & SHIREY, S. B. 2003. Mantle samples included in volcanic rocks: xenoliths and diamonds. In *Treatise on Geochemistry* (ed. R. W. Carlson), pp. 171–275. Oxford: Pergamon.

PEI, F. P., XU, W. L., WANG, Q. H., WANG, D. Y. & LIN, J. Q. 2004. Mesozoic basalt and mineral chemistry of the mantle-derived xenocrysts in Feixian, Western Shandong, China: Constraints on nature of Mesozoic lithospheric mantle. *Geological Journal of China Universities* **10**, 88–97 (in Chinese with English abstract).

REDFERN, S. A. T., HENDERSON, C. M. B., WOOD, B. J., HARRISON, R. J. & KNIGHT, K. S. 1996. Determination of olivine cooling rates from metal-cation ordering. *Nature* **381**, 407–9.

SCULLY, K. R., CANIL, D. & SCHULZE, D. J. 2004. The lithospheric mantle of the Archean Superior Province as imaged by garnet xenocryst geochemistry. *Chemical Geology* **207**, 189–221.

SHANXI BUREAU OF GEOLOGY AND MINERAL RESOURCES. 1982. *Regional geology of Shanxi Province*. Beijing: Geological Publishing House, 780 pp. (in Chinese with English abstract).

SHAO, J. A., LU, F. X., ZHANG, L. Q. & YANG, J. H. 2005. Discovery of xenocrysts in basalts of Yixian Formation in west Liaoning Province and its significance. *Acta Petrologica Sinica* **21**, 1547–58 (in Chinese with English abstract).

SUHR, G., HELLEBRAND, E., SNOW, J. E., SECK, H. A. & HOFMANN, A. W. 2003. Significance of large, refractory dunite bodies in the upper mantle of the Bay of Islands Ophiolite. *Geochemistry Geophysics Geosystems* **4**(3), 8605, doi:10.1029/2001GC000277.

TANG, Y. J., ZHANG, H. F. & YING, J. F. 2004. High-Mg olivine xenocrysts entrained in Cenozoic basalts in central Taihang Mountains: relics of old lithospheric mantle. *Acta Petrologica Sinica* **20**, 1243–52 (in Chinese with English abstract).

THOMPSON, R. N. & GIBSON, S. A. 2000. Transient high temperatures in mantle plume heads inferred from magnesian olivines in Phanerozoic picrites. *Nature* **407**, 502–6.

ULMER, P. 1989. The dependence of the Fe^{2+}–Mg cation-partitioning between olivine and basaltic liquid on pressure, temperature and composition – an experimental-study to 30 Kbars. *Contributions to Mineralogy and Petrology* **101**, 261–73.

WANG, Y. J., FAN, W. M., ZHANG, H. F. & PENG, T. P. 2006. Early Cretaceous gabbroic rocks from the Taihang Mountains: Implications for a paleosubduction-related lithospheric mantle beneath the central North China craton. *Lithos* **86**, 281–302.

WU, F. Y., WALKER, R. J., REN, X. W., SUN, D. Y. & ZHOU, X. H. 2003. Osmium isotopic constraints on the age of lithospheric mantle beneath northeastern China. *Chemical Geology* **196**, 107–29.

WU, F. Y., WALKER, R. J., YANG, Y. H., YUAN, H. L. & YANG, J. H. 2006. The chemical-temporal evolution of lithospheric mantle underlying the North China Craton. *Geochimica et Cosmochimica Acta* **70**, 5013–34.

XU, Y. G. 2001. Thermo-tectonic destruction of the Archaean lithospheric keel beneath the Sino-Korean craton in China: evidence, timing and mechanism. *Physics and Chemistry of Earth* **26**, 747–57.

XU, Y. G., BLUSZTAJN, J., MA, J. L., SUZUKI, K., LIU, J. F. & HART, S. R. 2008. Late Archean to Early Proterozoic lithospheric mantle beneath the western North China craton: Sr–Nd–Os isotopes of peridotite xenoliths from Yangyuan and Fansi. *Lithos* **102**, 25–42.

YAN, J., CHEN, J. F. & XIE, Z. 2003. Mantle derived xenoliths in the late Cretaceous basalts in eastern Shandong: new constraints on the timing of lithospheric thinning in east China. *Chinese Science Bulletin* **48**, 1570–4.

YING, J. F., ZHANG, H. F., KITA, N., MORISHITA, Y. & SHIMODA, G. 2006. Nature and evolution of Late Cretaceous lithospheric mantle beneath the eastern North China craton: Constraints from petrology and geochemistry of peridotitic xenoliths from Jünan, Shandong Province, China. *Earth and Planetary Science Letters* **244**, 622–38.

ZHANG, H. F., SUN, M., ZHOU, X. H., FAN, W. M., ZHAI, M. G. & YIN, J. F. 2002. Mesozoic lithosphere destruction beneath the North China craton: evidence from major-, trace-element and Sr–Nd–Pb isotope studies of Fangcheng basalts. *Contributions to Mineralogy and Petrology* **144**, 241–54.

ZHANG, H. F. 2005. Transformation of lithospheric mantle through peridotite-melt reaction: A case of Sino-Korean craton. *Earth and Planetary Science Letters* **237**, 768–80.

ZHANG, H. F., GOLDSTEIN, S., ZHOU, X. H., SUN, M., ZHENG, J. P. & CAI, Y. 2008. Evolution of subcontinental lithospheric mantle beneath eastern China: Re–Os isotopic evidence from mantle xenoliths in Paleozoic kimberlites and Mesozoic basalts. *Contributions to Mineralogy and Petrology* **155**, 271–93.

ZHANG, H. F., SUN, M., ZHOU, M. F. & FAN, W. M. 2004*a*. Highly heterogeneous late Mesozoic lithospheric mantle beneath the North China craton: evidence from Sr–Nd–Pb isotopic systematic of mafic igneous rocks. *Geological Magazine* **141**, 55–62.

ZHANG, H. F., YING, J. F., SHIMODA, G., KITA, N. T., MORISHITA, Y., SHAO, J. A. & TANG, Y. J. 2007. Importance of melt circulation and crust–mantle interaction in the lithospheric evolution beneath the North China Craton: Evidence from Mesozoic basalt-borne clinopyroxene xenocrysts and pyroxenite xenoliths. *Lithos* **96**, 67–89.

ZHANG, H. F., YING, J. F., XU, P. & MA, Y. G. 2004*b*. Mantle olivine xenocrysts entrained in Mesozoic basalts from the North China Craton: implication for replacement process of lithospheric mantle. *Chinese Science Bulletin* **49**, 961–6.

ZHAO, G. C., CAWOOD, P. A., WILDE, S. A., SUN, M. & LU, L. Z. 2000. Metamorphism of basement rocks in the Central Zone of the North China Craton: implications for Paleoproterozoic tectonic evolution. *Precambrian Research* **103**, 55–88.

ZHAO, G. C., WILDE, S. A., CAWOOD, P. A. & SUN, M. 2001. Archean blocks and their boundaries in the North China Craton: lithological, geochemical, structural and P–T

path constraints and tectonic evolution. *Precambrian Research* **107**, 45–73.

ZHENG, J. P. 1999. *Mesozoic–Cenozoic mantle replacement and lithospheric thinning, East China*. Wuhan: China University of Geosciences Press, 126 pp. (in Chinese with English abstract).

ZHENG, J. P., LU, F. X., GRIFFIN, W. L., YU, C. M., ZHANG, R. Y., YUAN, X. P. & WU, X. L. 2006. Lithospheric thinning accompanying mantle lateral spreading, erosion and replacement beneath the eastern part of North China: evidence from peridotites. *Earth Science Frontier* **13**, 76–85 (in Chinese with English abstract).

ZHENG, J. P., O'REILLY, S. Y., GRIFFIN, W. L., LU, F. X., ZHANG, M. & PEARSON, N. J. 2001. Relic refractory mantle beneath the eastern North China block: significance for lithosphere evolution. *Lithos* **57**, 43–66.